Selective Sodium Sensing with Gold-Coated Silicon Nanowire Field-Effect Transistors in a Differential Setup

Mathias Wipf,[†,*] Ralph L. Stoop,[†] Alexey Tarasov,[†] Kristine Bedner,[‡] Wangyang Fu,[†] Iain A. Wright,[§] Colin J. Martin,[§] Edwin C. Constable,[§] Michel Calame,[†] and Christian Schönenberger[†]

[†]Department of Physics, University of Basel, Basel, Switzerland, [‡]Laboratory for Micro- and Nanotechnology, Paul Scherrer Institut, Villigen, Switzerland, and [§]Department of Chemistry, University of Basel, Basel, Switzerland

ABSTRACT Ion-sensitive field-effect transistors based on silicon nanowires with high dielectric constant gate oxide layers (*e.g.*, Al_2O_3 or HfO_2) display hydroxyl groups which are known to be sensitive to pH variations but also to other ions present in the electrolyte at high concentration. This intrinsically nonselective sensitivity of the oxide surface greatly complicates the selective sensing of ionic species other than protons. Here, we modify individual nanowires with thin gold films as a novel approach to surface functionalization for the detection of specific analytes. We demonstrate sodium ion (Na^+) sensing by a self-assembled monolayer (SAM) of thiol-modified crown ethers in a differential measurement setup. A selective Na^+ response of ≈−44 mV per decade in a NaCl solution is achieved and tested in the presence of protons (H^+), potassium (K^+), and chloride (Cl^-) ions, by measuring the difference between a nanowire with a gold surface functionalized by the SAM (active) and a nanowire with a bare gold surface (control). We find that the functional SAM does not affect the unspecific response of gold to pH and background ionic species. This represents a clear advantage of gold compared to oxide surfaces and makes it an ideal candidate for differential measurements.

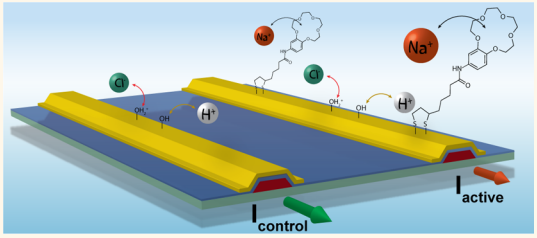

KEYWORDS: nanowire · sensing · anion adsorption · sodium · gold · ion-sensitive field-effect transistor

During the past decade, the principle of the ion-sensitive field-effect transistor (ISFET), proposed in the 1970s by Bergveld *et al.*,[1] experienced a revival at the nanoscale. A huge variety of possible sensor applications such as pH sensing[2−4] and chemical[5−10] and label-free biosensing[2,11−15] have been demonstrated by using silicon nanowire FETs (SiNWFETs). Further kinetic studies on receptor binding[16] and even intracellular recordings of action potentials[17] could be realized by downscaling of the devices. The sensing principle is based on adsorption of charged species on the sensor surface, leading to a change in surface potential and hence a change in current in the FET channel. Thereby, the high-impedance input signal is transformed into a low-impedance output signal, which is an advantage against classic ion-selective electrodes. The possibility of downscaling and integration[18] for the simultaneous detection of multiple parameters make SiNWFETs a promising platform to meet the demand for cheap, multifunctional, and scalable sensors.

Bare high-quality oxide surfaces have been shown to be very sensitive to proton concentration (pH).[4,19] Values close to the Nernst limit, which is the maximum possible shift in surface potential due to a change in pH ($\ln(10)kT/e$ = 59.5 mV/pH at 300 K), were obtained for Al_2O_3 and HfO_2. Oxide characteristics such as the number of surface hydroxyl groups and the reaction constants for protonation and deprotonation can be extracted with the site-binding model, as described in ref 20.

For the selective sensing of distinct species other than protons, the surface needs to be modified in such a way that only the targeted analyte is adsorbed. The covalent chemical anchoring of linker molecules has proven to be a viable method. Self-assembled monolayers (SAMs) exhibit the linker binding sites close to the FET surface at a high density. The field of SAMs has extensively been studied.[21] In ISFET systems, a widely used method is the self-assembly of silane monolayers to modify various types of oxide surfaces.[2,6,10]

* Address correspondence to mathias.wipf@unibas.ch.

Received for review April 5, 2013 and accepted June 14, 2013.

Published online June 14, 2013
10.1021/nn401678u

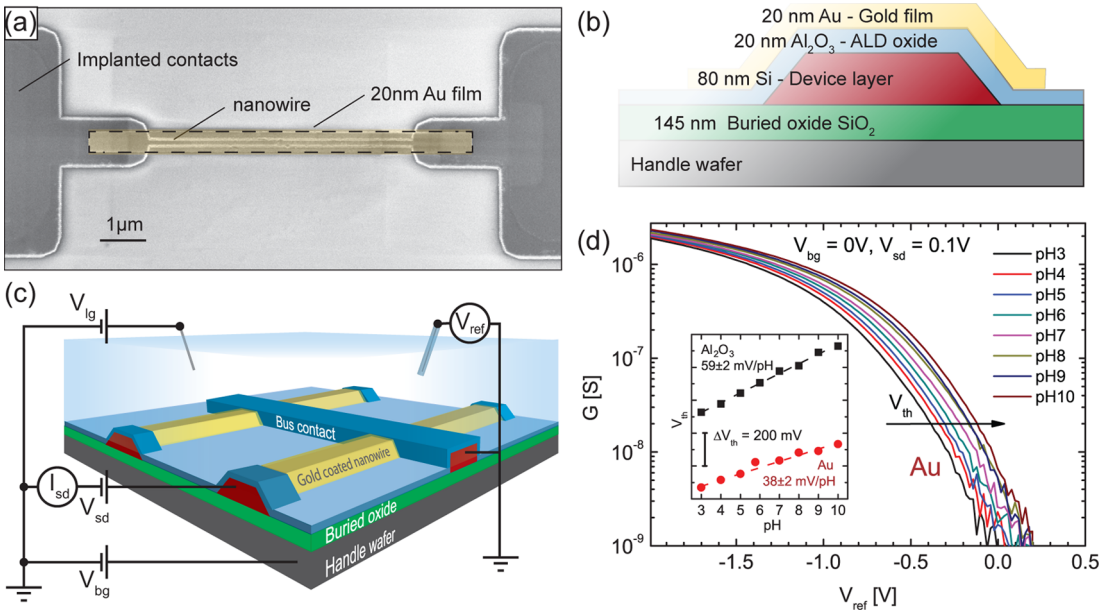

Figure 1. Device structure and measurement setup. (a) SEM micrograph of a 150 nm wide silicon nanowire coated with a 20 nm thick Al_2O_3 dielectric (by atomic layer deposition, ALD). NWs are lithographically defined in silicon on insulator wafers. Chromium (5 nm) as adhesion layer and gold (20 nm) are deposited on top of the nanowire by electron beam evaporation. Contact regions are highly p-doped. (b) Schematics of a nanowire cross section with the gold film covering the NWs. (c) Schematics of the measurement setup. A source meter is used to apply a source−drain voltage V_{sd} and to measure the source−drain current I_{sd}. Using a switching box, up to 48 NWs can be measured on one sample. The back-gate voltage V_{bg} is applied to the wafer substrate. The liquid-gate voltage V_{lg} is applied by a platinum wire immersed into the electrolyte. The liquid potential V_{ref} is measured by a calomel reference electrode. (d) Conductance curves G *vs* V_{ref} of a 250 nm wide gold-coated SiNW in different pH buffer solutions. The transfer curves shift to the right with increasing pH. The threshold voltage V_{th} is defined in the subthreshold regime at a constant conductance value of 20 μS (arrow). Inset: V_{th} at different pH for Al_2O_3 (59.5 mV/pH) and Au (38 mV/pH).

In this work, we cover SiNWFETs with a thin gold layer. Using a metal instead of an oxide surface enables new possibilities of surface chemistry to achieve selective sensing. We functionalize one-half of a sample with SAMs of sodium-selective crown ethers, whereas the other half remains untreated. Thereby, we obtain two groups of NWs with different surfaces: gold-coated NWs functionalized by the SAM (active NWs) and nonfunctionalized NWs with just a bare gold surface (control NWs). We demonstrate specific sodium ion sensing in a differential measurement. Measuring an active NW against a control NW leads to a response of ≈−44 mV/dec NaCl in the biologically relevant concentration range of 1−1000 mM. We find that the clean gold surface shows a response to protons and changes in the background ion concentration. We explain this behavior by the formation of gold oxide at the gold film surface[22−24] and its reaction with protons and chloride ions (Cl^-).[19,20] Interestingly, we find that the thiol−gold bonds of the SAM do not affect the number of oxidized gold atoms, thereby leaving the response of functionalized gold to pH and Cl^- unchanged. This is contrary to the behavior of oxide-coated devices where the functionalization does affect the pH response of the device.[20] Thanks to this special property of the gold surface, it is possible to compare active and control NWs directly, as realized by the proposed differential measurement.

RESULTS AND DISCUSSION

The samples were fabricated using p-doped silicon on insulator (SOI) wafers and a top-down fabrication process according to previously published protocols.[3,19,20,25] The samples, each containing 48 nanowires, were patterned by electron beam lithography and anisotropic wet etching. The nanowires are 6 μm in length, 85 nm in height, and of eight different defined widths, ranging from 100 nm to 1 μm. As gate oxide, 20 nm Al_2O_3 was deposited by atomic layer deposition (ALD). The high quality of the ALD oxide ensures low hysteresis and low leakage currents in the liquid. In addition, it exhibits a high density of surface hydroxyl groups, resulting in a maximum possible response of 59.5 mV/pH to a change in proton concentration, given by the Nernst limit.

For the gold-coated NWs, a 5 nm chromium adhesion layer and a 20 nm gold film was evaporated onto the Al_2O_3 dielectric layer. The SEM micrograph in Figure 1a shows the lateral dimensions of the gold film, highlighted by the dashed line, with respect to a NW. The gold area was lithographically defined and overlaps the NWs in length and width. Figure 1b shows the schematics of the cross section of a device, and Figure 1c shows a sketch of the measurement setup. Twelve NWs share a common bus line. A source meter (Keithley 2636A) is used to apply the source−drain

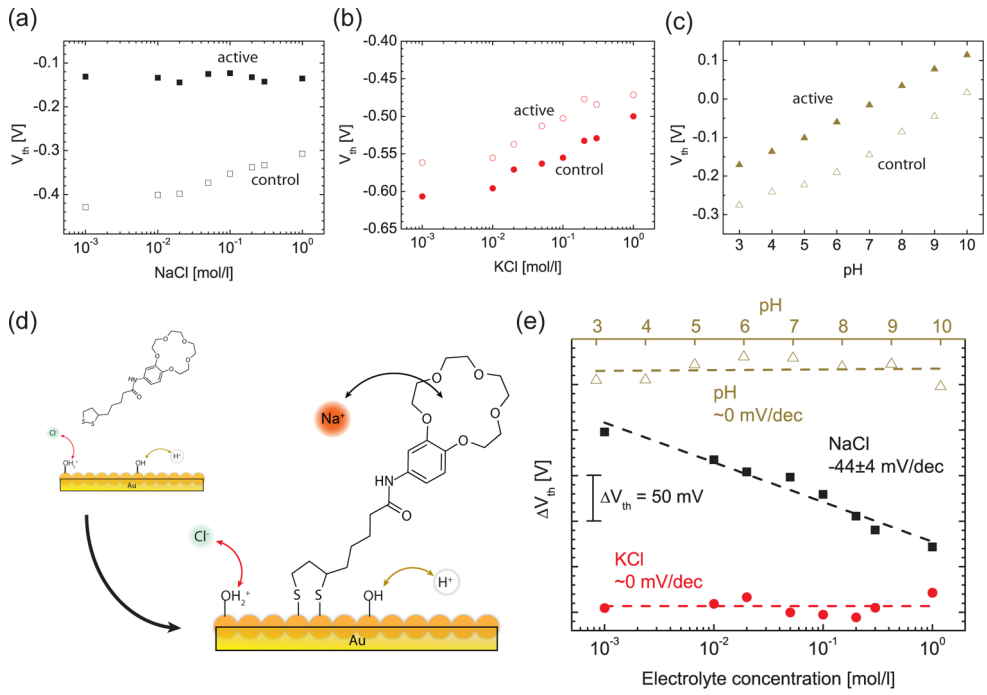

Figure 2. Surface functionalization with 15-crown-5 for Na^+ sensing. (a–c) V_{th} for a 1 μm wide functionalized (active) and 400 nm wide bare gold (control) NWs against c[NaCl] (a), c[KCl] (b), and pH (c). The response to NaCl changes with crown ether functionalization, whereas no difference between active and control NWs is seen when measuring in KCl and pH buffer solutions. (d) Immobilization reaction scheme of the sodium-selective crown ether on gold. We propose that the thiol only reacts with (reduced) gold atoms, leaving the number of hydroxyl groups unchanged. (e) Differential threshold voltage (ΔV_{th}) of gold-coated NWs (active 15-crown-5–control gold) *vs* the electrolyte concentration and pH. The crown ether shows high selectivity toward Na^+.

voltage V_{sd} (DC) and to measure the source–drain current I_{sd}. Using a switching box (Keithley 3706), up to 48 NWs can be measured on one sample. The back-gate potential V_{bg} is applied to the handle wafer. The liquid-gate V_{lg} is applied by a platinum wire immersed in the liquid. The actual liquid potential V_{ref} is measured by a calomel reference electrode.

Figure 1d shows the conductance *G versus* the liquid potential V_{ref} of a nanowire with a 20 nm thick gold film on top. With increasing pH, the transfer curve shifts to the right. To quantify the shift, we define the threshold voltage V_{th} at a fixed conductance value of 20 nS (indicated by the arrow). The inset shows the pH response of nanowires with different surface materials. Atomic layer deposited Al_2O_3 shows a linear response of 59 mV/pH, an effect induced by protonation and deprotonation of surface hydroxyl groups. This response close to the Nernst limit requires a high density of surface hydroxyl groups. Compared to such oxide surfaces, gold also shows a linear response but with a significantly smaller slope of ≈38 mV/pH. Furthermore, gold-coated NWs show a response to the ionic strength when measuring in NaCl and KCl solutions, similar to Al_2O_3 and HfO_2. As described recently,[19] we attribute this effect to the adsorption of chloride ions at the nanowire surface. No significant change of the response to protons and Cl^- has been observed over time. Even though gold is not expected to be corroded, the moderate response to protons indicates the formation of a gold oxide layer.[22–24] With a site-binding model for protonation, deprotonation, and Cl^- adsorption described in refs 19 and 20, we estimate the number of hydroxylated gold surface atoms to be only ≈1%. A detailed characterization of the gold surface and the estimation of the hydroxyl group density is given in the Methods section.

Sodium Sensing. Preparing self-assembled monolayers of organic molecules at surfaces is an effective functionalization process for chemical sensing. Functional groups designed for trapping specific analytes can be immobilized close to the surface in this way. Crown ethers, consisting of a ring containing several ether groups, strongly bind cations due to the negatively polarized oxygen atoms. The selectivity to the type of ion can be controlled by varying the number of ether groups and the cavity diameter.[26] Here we used a Na^+-selective 15-crown-5 functionalized with a dithiolane anchoring moiety (Figure 2d). The samples were cleaned in oxygen plasma and closed with a PDMS microchannel. The samples were divided in two (active and control) parts by individual channels in the PDMS. The wires in the active channel were then functionalized with the 15-crown-5. This results in a differential setup having both NWs with functionalized gold surface (active NWs) and bare gold-coated NWs (control NWs) on the same chip.

Figure 2a shows the response of an active and a control NW to NaCl. For the control NW, we find a positive shift in V_{th} with increasing salt concentration due to adsorption of Cl^- on the gold surface. The immobilization of the 15-crown-5 changes this response: instead of the positive shift, a slightly negative shift is observed for the active NW, indicating adsorption of positive charges on the surface. The differential signal ($\Delta V_{th} = V_{th,active} - V_{th,control}$) shown in Figure 2e shows a response to NaCl of ≈ -44 mV/dec. Control measurements with KCl in Figure 2b show no difference between bare and functionalized gold, suggesting a high selectivity of the 15-crown-5 toward Na^+ and none for K^+. In the case of pH response (Figure 2c), the two different surfaces behave the same way. The differential signal (ΔV_{th}) in Figure 2e emphasizes that only a change in Na^+ concentration induces a different response of the two surfaces. Thus a good Na^+ sensor with high response and specificity was realized. Further it indicates that protonation and deprotonation of surface hydroxyl groups, as well as their interaction with Cl^- is unaffected by the self-assembly of the crown ethers. In Figure 2d, we propose a functionalization scheme where the sulfur–gold binding only happens at non-oxidized gold atoms ($\approx$99% of the surface), leaving the number of hydroxyl groups unchanged.[23] It is our picture that the crown ether functionalization adds a third type of surface reaction to the system, without affecting the number of hydroxyl groups and their interaction with the electrolyte. Thus, the response of 15-crown-5 is a superposition of the positive shift coming from Cl^- adsorption at $-OH_2^+$ sites and Na^+ reacting with the crown ether. Subtracting the signal of a control gold-coated NW from an active NW (ΔV_{th}) reveals the response of the crown ether.

CONCLUSION

In conclusion, we demonstrate a selective cation sensing by the self-assembly of Na^+-selective crown ethers on gold-coated NWs. In a differential measurement with active and control NWs on the same chip, a response of ≈ -44 mV/dec in the concentration range of 1 mM up to 1 M was achieved. The response to NaCl is more than an order of magnitude larger than that for KCl, indicating good selectivity. We showed that gold surfaces are slightly sensitive to changes in proton and Cl^- concentration. Both effects indicate the small density of hydroxyl groups at the gold surface. We infer from our measurements that the thiol–gold binding during the SAM formation happens only at non-oxidized gold atoms, leaving the number of hydroxyl groups unchanged. As a consequence, the thiol functionalization of gold does not affect the pH sensitivity and the response to Cl^-.

Our results underline the importance of monitoring the changes in pH and ionic strength simultaneously for specific ion-detection experiments. It enables the distinction of the signal caused by the target analyte and the contributions of the background electrolyte. In this work, this is realized by the differential measurement setup using the nonfunctionalized control gold surface as a proton and chloride-sensitive reference electrode. However, the influence of the background electrolyte only cancels out in the differential signal if the functionalization does not change the response to any analyte except the targeted one. In this respect, the gold surface appears to be an ideal candidate.

METHODS

Device Fabrication. The samples were produced by a top-down approach described in a previously published protocol.[20] Silicon on insulator (SOI) wafers (Soitec, France) with a buried oxide (BOX) layer of 145 nm in thickness were used. The 85 nm thick p-Si(100) device layer with a resistivity of 8.5–11.5 Ω·cm was oxidized thermally until a 15 nm thick SiO_2 layer was grown. The nanowire pattern was defined by electron beam lithography (EBL). The nanowires were then carved out by dry etching of SiO_2 and anisotropic wet etching of the Si device layer with tetramethylammonium hydroxide (TMAH and isopropyl alcohol 9:1 at 45°). The resulting NW with Si(111) side faces were 6 μm long, 80 nm high, and 100–1000 nm wide. The source and drain contact areas were heavily doped by BF_2^+ ions (energy = 33 keV, dose 2.3×10^{15} cm^{-2}). The dopants were activated by thermal annealing in a forming gas (6 min at 950 °C). Afterward, the 22 nm Al_2O_3 dielectric was deposited by atomic layer deposition (ALD) at 225 °C (Savannah S100, Cambridge NanoTech). The ohmic contacts were metallized by Al–Si(1%) and annealed at 450 °C after local etching of the ALD oxide. A 2 μm thick protection layer (SU-8 2002, MicroChem) with 6 μm wide openings (aligned to the NWs), defined by UV lithography, was used as liquid protection. To operate the samples in liquid, they were wire bonded into a chip carrier. The bonds were sealed with epoxy (Epotek 353ND).

Microchannels. Microchannels were produced by pouring polydimethylsiloxane (PDMS, SYLGARD 184 Silicone Elastomer) onto SU-8 (SU-8 100 MicroChem) patterned Si wafers, degassing, and heating at 60 °C for 2 h. Polytetrafluoroethylene (PTFE) tubes were used to connect the microchannels to a peristaltic pump and the electrolyte solutions.

Surface Functionalization. For immobilization of thiol-terminated 15-crown-5, one-half of the NWs on a sensor chip were covered with 5 nm chromium as adhesion layer and 20 nm gold by e-beam evaporation. The samples were cleaned in O_2 plasma (Oxford Plasmalab 80 plus, 30 W, 45 s) and covered with a PDMS microchannel. The 15-crown-5 molecule was synthesized as described in the Supporting Information and dissolved in ethanol ($\approx$2 mM). The SAMs were obtained by pumping the solution through the (active) microchannels with long stabilization intervals for 16 h. After the functionalization, the channels were rinsed with ethanol and deionized water.

Electrical Measurements in Liquid. Standard pH buffer solutions were used for the pH measurement (Titrisol, Merck). KCl (ACS 99.0–100.5%, Alfa Aesar) and NaCl ($\geq$99.5%, Fluka) were dissolved in deionized water (resistivity = 17 MΩ·cm), resulting in a pH value around 6.

A peristaltic pump (MCP, Ismatec) and a valve selector system (CHEMINERT VICI, Valco Instruments Co. Inc.) were used to exchange the solutions. Prior to a measurement series, the samples were left in contact with the solution for $\approx$1 h to

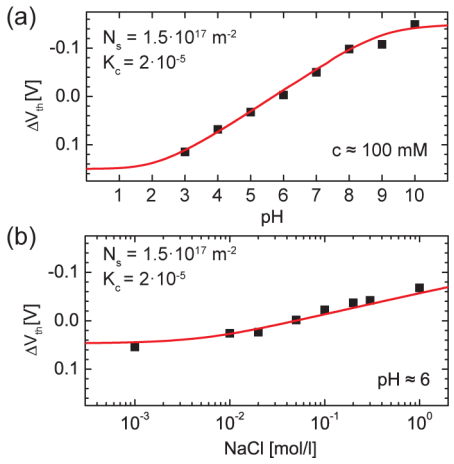

Figure 3. Response to pH and ionic strength of a gold-coated NW (solid squares) fitted with a combined site-binding model for protonation, deprotonation, and Cl^- adsorption (red lines). (a) Change in threshold voltage ΔV_{th} *vs* pH of a 250 nm wide wire. From the pH response, the number of active hydroxyl groups N_s is estimated to be 1.5×10^{17} m^{-2}, which is a factor 60 less than for a Al_2O_3 surface. (b) ΔV_{th} *vs* c[NaCl] for a 300 nm wide wire. Although the number of hydroxyl groups on gold is significantly lower than on Al_2O_3, a pronounced response to Cl^- is still observed for gold. Taking the obtained N_s to fit our chloride adsorption model to the response of gold to NaCl yields a reaction constant for Cl^- adsorption $K_c = 2 \times 10^{-5}$.

stabilize the sensor/electrolyte interface. After changing the solutions, the samples were stabilized for a few minutes before each measurement. During a measurement, the liquid potential, controlled by the reference electrode, was changed, while the NW conductance was measured at constant source−drain voltage V_{sd} = 100 mV (Keithley 2636A). Using a switching box (Keithley 3706), up to 48 NWs were measured. During the whole measurement V_{bg} was fixed at a constant voltage. All devices were automatically controlled by a self-made LabView program. Two different types of liquid setups were used. A liquid cell where the liquid-gate was applied to a platinum or gold wire and the potential was measured with a calomel reference electrode (REF200, Radiometer analytical) (Figure 1d and Figure 3a), as well as PDMS microchannels where the liquid potential was directly applied to a flow-through Ag/AgCl reference electrode (Microelectrodes, Inc.) embedded in the PTFE tubing (Figure 2 and Figure 3b).

Characterization of the Gold Surface. Figure 3 shows the response of a gold-coated NW to changes in pH and NaCl. The vertical axis shows the shift in threshold voltage (ΔV_{th}). This corresponds to the difference in surface potential ($-\Delta\Psi$) since a p-type semiconductor was used. To quantify the number of hydroxyl groups of the gold oxide, we use the full site-binding model described in refs 20 and 27−29 and the model for anion adsorption by positively charged hydroxyl groups described in ref 19.

The following expressions describe the reactions at the gold surface. Due to the amphoteric character of the OH surface groups of the metal oxide surface, two reaction constants for deprotonation (K_a) and protonation (K_b) are needed. A third reaction constant (K_c) describes the Cl^- adsorption.

$$MOH \rightleftharpoons MO^- + H_s^+, K_a = \frac{v_{MO^-} a_{H_s^+}}{v_{MOH}} \quad (1)$$

$$MOH_2^+ \rightleftharpoons MOH + H_s^+, K_b = \frac{v_{MOH} a_{H_s^+}}{v_{MOH_2^+}} \quad (2)$$

$$MOH_2^+ + Cl_s^- \rightleftharpoons MOHCl^- + H_b^+, K_c = \frac{v_{MOHCl^-} a_{H_b^+}}{v_{MOH_2^+} a_{Cl_s^+}} \quad (3)$$

Indices s and b denote surface and bulk; $a_{H_s^+}$ is the activity of the surface protons and v is the number of sites per m^2 for one particular species. The total number of sites per m^2 is

$$N_s = v_{MOH} + v_{MO^-} + v_{MOH_2^+} + v_{MOHCl^-} \quad (4)$$

The resulting surface charge density σ_0 is screened by the double-layer capacitance per m^2 C_{dl} leading to the surface potential drop Ψ

$$\Psi = \frac{\sigma_0}{C_{dl}}, \sigma_0 = e(v_{MOH_2^+} - v_{MO^-} - v_{MOHCl^-}) \quad (5)$$

The parameters were set as follows: $K_a = K_b = 10^{-7}$, $C_{dl} = 0.16$ F/m^2 according to refs 19 and 20. Protonation and deprotonation are equally probable ($K_a = K_b$). Otherwise, a double s-shaped response would be expected, as exemplified in ref 20. C_{dl} can be taken as a fixed value since it is dominated by the Stern layer capacitance which is independent of the ionic strength. Fitting the response of gold to pH and ionic strength with our combined site-binding model for Cl^- adsorption (red lines in Figure 3) results in an estimated surface hydroxyl group density $N_s = 1.5 \times 10^{17}$ m^{-2} and a reaction constant $K_c \approx 2 \times 10^{-5}$. Here N_s is ≈60 times smaller for Au than for Al_2O_3. Although only few gold surface atoms (≈1%) are oxidized, the s-shaped response to pH with a linear behavior between pH 4 and 8 of ≈40 mV/pH is well described by this site-binding model. K_c is roughly 7 times larger than the value found for Al_2O_3 and HfO_2.[19] This affects the response to Cl^-, where the threshold of the linear region is shifted to lower electrolyte concentration.

Conflict of Interest: The authors declare no competing financial interest.

Acknowledgment. The authors gratefully acknowledge the support by the Swiss Nanoscience Institute (SNI), the Swiss Nano-Tera program, Sensirion AG, and the European Commission under the FP7-NMP project Hysens (263091).

Supporting Information Available: Synthesis of 15-crown-5 and molecule details are are available as Supporting Information. This material is available free of charge *via* the Internet at http://pubs.acs.org.

REFERENCES AND NOTES

1. Bergveld, P. Development of an Ion-Sensitive Solid-State Device for Neurophysiological Measurements. *IEEE Trans. Biomed. Eng.* **1970**, *BME-17*, 70–71.
2. Cui, Y.; Wei, Q.; Park, H.; Lieber, C. M. Nanowire Nanosensors for Highly Sensitive and Selective Detection of Biological and Chemical Species. *Science* **2001**, *293*, 1289–1292.
3. Knopfmacher, O.; Tarasov, A.; Fu, W.; Wipf, M.; Niesen, B.; Calame, M.; Schönenberger, C. Nernst Limit in Dual-Gated Si-Nanowire FET Sensors. *Nano Lett.* **2010**, *10*, 2268–2274.
4. Chen, S.; Bomer, J. G.; Carlen, E. T.; van den Berg, A. Al_2O_3/Silicon NanoISFET with near Ideal Nernstian Response. *Nano Lett.* **2011**, *11*, 2334–2341.
5. Janata, J. Chemical Sensors. *Anal. Chem.* **1992**, *64*, R196–R219.
6. Sudhölter, E.; van der Wal, P.; Skowronska-Ptasinska, M.; van den Berg, A.; Reinhoudt, D. Ion-Sensing Using Chemically-Modified ISFETs. *Sens. Actuators* **1989**, *17*, 189–194.
7. Rocher, V.; Jaffrezic-Renault, N.; Perrot, H.; Chevalier, Y.; Perchec, P. L. Nitrate-Sensitive Field-Effect Transistor with Silica Gate Insulator Modified by Chemical Grafting. *Anal. Chim. Acta* **1992**, *256*, 251–255.
8. Reinhoudt, D. N.; Engbersen, J. F. J.; Brzozka, Z.; van der Vlekkert, H. H.; Honig, G. W. N.; Holterman, H. A. J.; Verkerk, U. H. Development of Durable K^+-Selective Chemically Modified Field Effect Transistors with Functionalized Polysiloxane Membranes. *Anal. Chem.* **1994**, *66*, 3618–3623.
9. Park, L.; Hur, Y.; Sohn, B. Effect of Membrane Structure on the Performance of Field-Effect Transistor Potassium-Sensitive Sensor. *Sens. Actuators, A* **1996**, *57*, 239–243.
10. Luo, L.; Jie, J.; Zhang, W.; He, Z.; Wang, J.; Yuan, G.; Zhang, W.; Wu, L. C. M.; Lee, S.-T. Silicon Nanowire Sensors for Hg^{2+} and Cd^{2+} Ions. *Appl. Phys. Lett.* **2009**, *94*, 193101.

11. Gao, A.; Lu, N.; Wang, Y.; Dai, P.; Li, T.; Gao, X.; Wang, Y.; Fan, C. Enhanced Sensing of Nucleic Acids with Silicon Nanowire Field Effect Transistor Biosensors. *Nano Lett.* **2012**, *12*, 5262–5268.
12. Zheng, G.; Patolsky, F.; Cui, Y.; Wang, W. U.; Lieber, C. M. Multiplexed Electrical Detection of Cancer Markers with Nanowire Sensor Arrays. *Nat. Biotechnol.* **2005**, *23*, 1294–1301.
13. Stern, E.; Klemic, J. F.; Routenberg, D. A.; Wyrembak, P. N.; Turner-Evans, D. B.; Hamilton, A. D.; LaVan, D. A.; Fahmy, T. M.; Reed, M. A. Label-Free Immunodetection with CMOS-Compatible Semiconducting Nanowires. *Nature* **2007**, *445*, 519–522.
14. Stern, E.; Vacic, A.; Rajan, N. K.; Criscione, J. M.; Park, J.; Ilic, B. R.; Mooney, D. J.; Reed, M. A.; Fahmy, T. M. Label-Free Biomarker Detection from Whole Blood. *Nat. Nanotechnol.* **2010**, *5*, 138–142.
15. Elfström, N.; Karlström, A. E.; Linnros, J. Silicon Nanoribbons for Electrical Detection of Biomolecules. *Nano Lett.* **2008**, *8*, 945–949.
16. Duan, X.; Li, Y.; Rajan, N. K.; Routenberg, D. A.; Modis, Y.; Reed, M. A. Quantification of the Affinities and Kinetics of Protein Interactions Using Silicon Nanowire Biosensors. *Nat. Nanotechnol.* **2012**, *7*, 401–407.
17. Duan, X.; Gao, R.; Xie, P.; Cohen-Karni, T.; Qing, Q.; Choe, H. S.; Tian, B.; Jiang, X.; Lieber, C. M. Intracellular Recordings of Action Potentials by an Extracellular Nanoscale Field-Effect Transistor. *Nat. Nanotechnol.* **2012**, *7*, 174–179.
18. Rothberg, J. M.; Hinz, W.; Rearick, T. M.; Schultz, J.; Mileski, W.; Davey, M.; Leamon, J. H.; Johnson, K.; Milgrew, M. J.; Edwards, M.; *et al.* An Integrated Semiconductor Device Enabling Non-optical Genome Sequencing. *Nature* **2011**, *475*, 348–352.
19. Tarasov, A.; Wipf, M.; Stoop, R. L.; Bedner, K.; Fu, W.; Guzenko, V. A.; Knopfmacher, O.; Calame, M.; Schönenberger, C. Understanding the Electrolyte Background for Biochemical Sensing with Ion-Sensitive Field-Effect Transistors. *ACS Nano* **2012**, *6*, 9291–9298.
20. Tarasov, A.; Wipf, M.; Bedner, K.; Kurz, J.; Fu, W.; Guzenko, V. A.; Knopfmacher, O.; Stoop, R. L.; Calame, M.; Schönenberger, C. True Reference Nanosensor Realized with Silicon Nanowires. *Langmuir* **2012**, *28*, 9899–9905.
21. Ulman, A. Formation and Structure of Self-Assembled Monolayers. *Chem. Rev.* **1996**, *96*, 1533–1554.
22. Lohrengel, M.; Schultze, J. Electrochemical Properties of Anodic Gold Oxide Layers-I: Potentiostatic Oxide Growth and Double Layer Capacity. *Electrochim. Acta* **1976**, *21*, 957–965.
23. Ron, H.; Rubinstein, I. Alkanethiol Monolayers on Preoxidized Gold. Encapsulation of Gold Oxide under an Organic Monolayer. *Langmuir* **1994**, *10*, 4566–4573.
24. Ron, H.; Matlis, S.; Rubinstein, I. Self-Assembled Monolayers on Oxidized Metals. 2. Gold Surface Oxidative Pretreatment, Monolayer Properties, and Depression Formation. *Langmuir* **1998**, *14*, 1116–1121.
25. Knopfmacher, O.; Tarasov, A.; Wipf, M.; Fu, W.; Calame, M.; Schönenberger, C. Silicon-Based Ion-Sensitive Field-Effect Transistor Shows Negligible Dependence on Salt Concentration at Constant pH. *ChemPhysChem* **2012**, *13*, 1157–1160.
26. Steed, J.; Atwood, J. *Supramolecular Chemistry*; John Wiley & Sons: New York, 2009.
27. Yates, D. E.; Levine, S.; Healy, T. W. Site-Binding Model of the Electrical Double Layer at the Oxide/Water Interface. *J. Chem. Soc., Faraday Trans.* **1974**, *70*, 1807–1818.
28. Healy, T. W.; White, L. R. Ionizable Surface Group Models of Aqueous Interfaces. *Adv. Colloid Interface Sci.* **1978**, *9*, 303–345.
29. Bousse, L.; De Rooij, N.; Bergveld, P. Operation of Chemically Sensitive Field-Effect Sensors as a Function of the Insulator-Electrolyte Interface. *IEEE Trans. Electron Devices* **1983**, *30*, 1263–1270.